PCCP

Accepted Manuscript

ROYAL SOCIETY OF CHEMISTRY

www.rsc.org/pccp

Lyotropic Liquid Crystal Phases of Phytantriol in a Protic Ionic Liquid with Fluorous Anion

Yan Shen,[a,b] *Tamar L. Greaves,*[a,d] *Danielle F. Kennedy,*[a] *Asoka Weerawardena,*[a,d] *Nigel Kirby,*[c] *Gonghua Song,*[b] *and Calum J. Drummond*[a,d*]

[a] CSIRO Materials Science and Engineering (CMSE), Bag 10, Clayton, Vic. 3169, Australia.
[b] Shanghai Key Laboratory of Chemical Biology, School of Pharmacy, East China University of Science and Technology, Shanghai 200237, PR China.
[c] Australian Synchrotron, 800 Blackburn Road, Clayton, Vic. 3168, Australia.
[d] School of Applied Sciences, College of Science, Engineering and Health, RMIT University, GPO Box 2476, Melbourne, Victoria 3001, Australia.
[*] Corresponding author. Email: calum.drummond@rmit.edu.au

Abstract

The phase behaviour of phytantriol in the protic ionic liquid (PIL) 1-methylimidazolium pentadecafluorooctanoate (MImOF) and four different MImOF-water compositions was investigated by small- and wide- angle X-ray scattering (SAXS/WAXS), cross polarised optical microscopy (CPOM) and infrared spectroscopy (IR). MImOF is an unusual protic ionic liquid in that it contains a fluorocarbon anion and a hydrocarbon cation. This leads to MImOF having an unusual liquid nanostructure, such that it contains fluorocarbon, hydrocarbon and polar domains. No lyotropic liquid crystal phases were observed for phytantriol in neat MImOF. However, on addition of water, lamellar, cubic Ia$\bar{3}$d and micellar phases were observed for specific MImOF-phytantriol-water compositions at room temperature, and up to 60 ^{o}C. The phase behaviour for phytantriol in the solvent mixture of 25wt%-MImOF/75 wt%-water was the most similar to the phytantriol-water phase diagram. Only this MImOF-water composition supported the Ia$\bar{3}$d cubic phase, which had a lattice parameter between 100-140 Å compared to 86-100 Å in deionised water[1], indicating significant swelling due to the MImOF. IR spectroscopy showed that a percentage of the water molecules were hydrogen bonded to the N-H of the MIm cation, and this water decreased the hydrogen bonding present between the cation and anion of the ionic liquid. This investigation furthers our understanding of the interaction of ionic liquids with solutes, and the important role that the different IL nanostructures can have on influencing these interactions.

Introduction

Protic ionic liquids (PILs) are a class of ionic liquids (ILs) which are produced through proton transfer from a Brønsted acid to a Brønsted base, and contain hydrogen bond donor and acceptor sites.[2] Many PILs, like other ILs, form polar and non-polar domains through segregation of the alkyl chain into non-polar domains.[3-5] The nanostructure of an IL is modified through the addition of other solvents or solutes, though there have been limited studies to date. Polar solutes, such as water, reside predominantly in the polar domain of the IL which is constituted by the cation headgroups and anions.[6,7] Solutes which contain both polar and non-polar moieties, such as primary alcohols, intercalate with the cations[8]. It is proposed that the interactions between ILs and solutes will have a significant impact

on their use in many applications, for example by modifying the solubility of various solutes, influencing the viscosity, having non-homogeneous distribution of solutes, influencing the self-assembly of amphiphiles[9], and as templating domains for the synthesis of nanoparticles[10].

Recently, fluorous protic ionic liquids which consist of a fluorous anion and a hydrocarbon cation (FPILs) have been reported.[11] The chemical structure of one of these FPILs, namely 1-methylimidazolium pentadecafluorooctanoate (MImOF), is provided in Figure 1a. The FPILs were shown to contain an unusual discrete nanostructure, possessing a hydrocarbon, fluorocarbon and polar domain[11]. Since then, analogous aprotic ILs have been reported, though their fluorocarbon domain is only present at low temperatures.[12] The good thermal stability of the FPIL fluorocarbon domain has been attributed to the stabilising effect of the hydrogen bonding present.[12] However, the more complicated structure of FPILs leads to significantly different behaviour, with for example the addition of primary alcohols leading to the formation of nano-scaled objects.[13] It is currently unknown how these FPILs will interact with more complicated solutes, such as amphiphiles.

In some ways, these FPILs and analogous aprotic ILs are similar to the star-polyphile surfactants which have been investigated by Hyde et al., which contain fluorous, hydrocarbon and polar components.[14] The star-polyphile surfactants can self-assemble in water to form liquid crystal phases which contain three distinct hydrophilic, oleophilic and fluorophilic domains.

It has previously been established that many PILs are capable of supporting amphiphile self-assembly into liquid crystal phases through the ‘‘solvophobic effect’’, analogous to the hydrophobic effect in water.[9,15-17] It was unknown whether this same phenomenon would occur for the more complex FPILs. We have selected phytantriol as an amphiphile to investigate with FPILs due to its well established self-assembly phase behaviour in water being well characterised[1], that tertiary systems consisting of phytantriol, water and a second solvent or second surfactant have previously been reported,[18,19] and also that the self-assembly of phytantriol in a variety of PILs has been reported [20-22]. In addition the hydrogen bonding in phytantriol has previously been investigated using Raman and FTIR combined with molecular modelling.[23] The chemical structure of phytantriol is provided in Figure 1b.

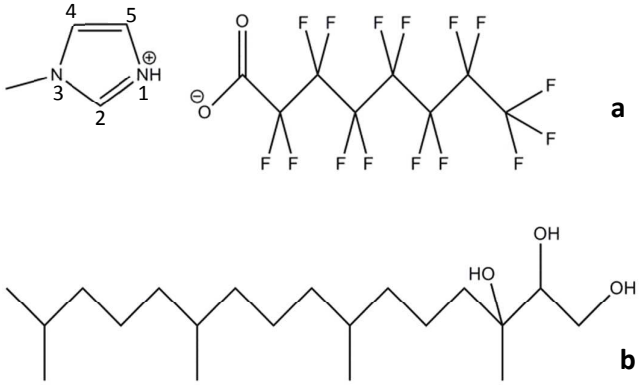

Figure 1. Chemical structure of a) MImOF and b) phytantriol.

Phytantriol is a small non-ionic amphiphile which can self-assembly into inverse micellar, lamellar, cubic phase Ia$\bar{3}$d, and cubic phase Pn$\bar{3}$m and an inverse hexagonal phase.[1] Cubic, lamellar and inverse hexagonal phases have been reported from phytantriol self-assembly in PILs, though there was less phase diversity in the PILs compared to water with only one or two phases observed in each PIL over a temperature range of 25 to 75 ^{o}C. A more detailed investigation showed that phytantriol formed the Ia$\bar{3}$d cubic mesophase in the PIL ethanolammonium formate (EAOF) at 25 ^{o}C.[22]

The prominent IR spectroscopy bands present for phytantriol in water have previously been reported, focussing on the those associated with hydrogen bonding and inter-chain interactions.[23] In addition, IR spectroscopy has been used to characterise IL-solute interactions, such as the addition of water[24], and the addition of water or methanol to butylmethylimidazolium trifluoroacetate [BMIm][CF_3CO_2] or ethylmethylimidazolium ethylsulfate [EMIm][$EtSO_4$] [25,26].

In this investigation we have explored the addition of phytantriol to neat MImOF, and to MImOF-water solutions which contain 10, 25, 50 or 75 wt% MImOF. We have also characterised the nanostructure of the MImOF-water solutions using synchrotron small and wide angle X-ray scattering SAXS/WAXS. The phytantriol liquid crystal phases were identified and characterised using cross-polarised optical microscopy (CPOM) and SAXS/WAXS. Infrared spectroscopy was used to explore the changes in the hydrogen-bonding present in the system.

Experimental Method

All chemicals were used as supplied. The phytantriol was used as received (Aldrich, 96% purity). 1-methylimidazolium pentadecafluorooctanoate (MImOF) was prepared as previously reported.[1] MImOF–water solutions were prepared from dried MImOF and deionised MiliQ water at concentrations of 10, 20, 25, 30, 40, 50, 60, 70, 75, 80 or 90 wt% water.

Small- and wide-angle X-ray scattering experiments were performed on the SAXS/WAXS beamline at the Australian Synchrotron, Clayton, Australia[27,28]. SAXS patterns were acquired for each of the MImOF-water compositions. In addition, six concentrations of phytantriol, namely 30, 40, 50, 60, 70 and 80 wt%, in neat MImOF and MImOF-water systems (90%-10%, 75%-25%, 50%-50% and 25%-75% wt%), were prepared. All samples were equilibrated for at least two weeks at room temperature before analysis. Samples were loaded into 2 mm glass capillaries, and sealed with silicon rubber to prevent water absorption. Samples were housed in a 60 sample capillary holder and mounted on a 3-axis sample stage. During analysis, all samples were heated from 25 to 70 ^{o}C in 5 ^{o}C increments. An exposure of 2 seconds was taken for each sample at each temperature. The temperature of the sample holder was controlled using a Huber recirculating water bath. SAXS and WAXS patterns were simultaneously acquired for all the samples. The SAXS q range was 0.044 to 0.86 Å^{-1}, and the WAXS q range was 0.69 to 2.52 Å^{-1}. The SAXS and WAXS profiles were combined to obtain profiles over the range from 0.044 to 2.52 Å^{-1}. The SAXS and WAXS patterns had an overlapping q region which was used to scale the WAXS intensity to the SAXS intensity to account for differences in sensitivity between the detectors. The scattering contribution from an empty capillary was subtracted from the scattering profiles. The capillaries were nominally 2 mm diameter; however, there were some small

deviations in size at the point of analysis, which lead to changes in the intensities of a few percent between samples.

The 2-D scattering patterns for both SAXS and WAXS were converted into 1-D scattering curves using SAXS15-id software provided at the Australian Synchrotron. The determination of the lyotropic liquid crystalline mesophases was based on the characteristic ratio of the Bragg diffraction peaks.

Penetration scans were conducted using cross polarised optical microscopy (CPOM) coupled with a temperature controller (with an upper temperature limit of 100 ^{o}C) to examine the phase behaviour of the phytantriol in neat MImOF and MImOF-water systems. The samples were prepared and analysed as detailed in the literature.[20]

Infrared spectroscopy measurements were made on a Nicolet 6700 FTIR using a diamond ATR attachment.

Results

The lyotropic liquid crystal phases present for phytantriol in neat MImOF, and MImOF-water solutions were investigated using a combination of SAXS/WAXS, cross-polarised optical microscopy (CPOM) and IR spectroscopy. Phytantriol concentrations of 30, 40, 50, 60, 70 and 80 wt% were used, in conjunction with solvent mixtures of MImOF-water containing 0, 10, 25, 50 or 75 wt% water. MImOF-water solvent mixtures without phytantriol were characterised to determine their contribution to the total nanostructure.

Neat MImOF and MImOF-water solvent mixtures

The combined SAXS and WAXS patterns for neat MImOF are shown in Figure 2. The pattern indexes well to a crystalline hexagonal phase with peak positions at $1:\sqrt{3}:\sqrt{4}:\sqrt{7}$ ... and a lattice spacing of 17.4 Å. The presence of strong diffraction peaks into the WAXS region clearly show that this sample is crystalline, which is consistent with its melting point of 86 ^{o}C.[11]

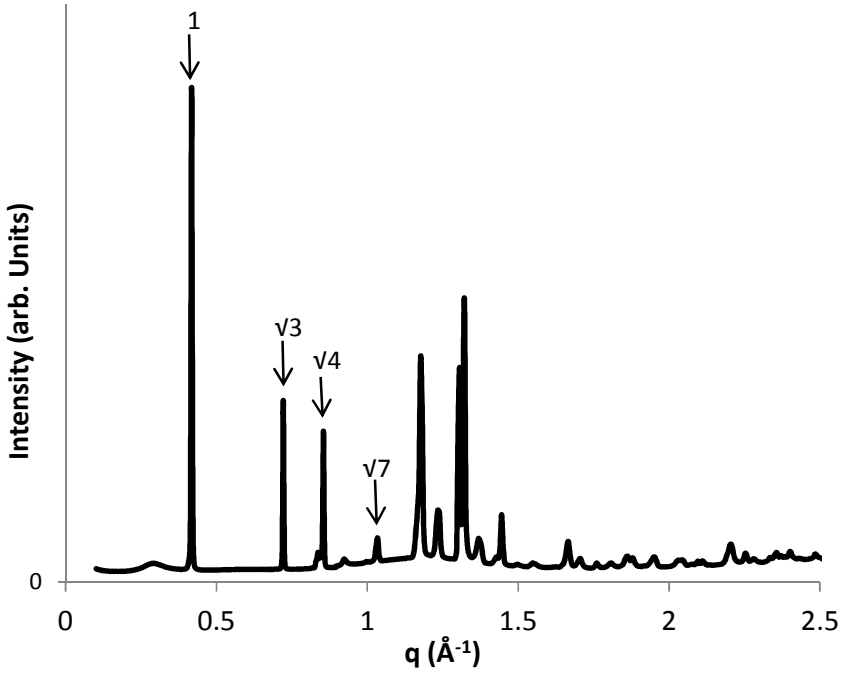

Figure 2. Combined SAXS and WAXS patterns for neat MImOF.

Solutions of MImOF-water were prepared with water concentrations between 10 and 90 wt% and their corresponding SAXS patterns are shown in Figure 3a. The WAXS patterns were not included since the samples were all non-crystalline with only a weak broad peak around 1.2 $Å^{-1}$ in the WAXS region. The prominent scattering peak at 0.25 $Å^{-1}$ shifts to the left (lower q) and increases in intensity with increasing water concentration, indicating that the size, or repeat spacing and the persistence of the repeating unit, is increasing with increasing water content. An additional weaker peak at 0.4 $Å^{-1}$ was present for most of the samples, as shown in Figure 3b for MImOF with 10 wt% water. For this sample shown the two broad peaks are present at 0.23 and 0.46 $Å^{-1}$, suggesting a disordered lamellar-like, or sponge-like phase, such as those which have previously been reported for PILs[7], where the broadness of the peaks indicates that it is not a well ordered phase. The intensity of the weaker peak decreased relative to the most prominent peak with increasing water content. More detailed investigations will be conducted in the future on FPIL-water interactions.

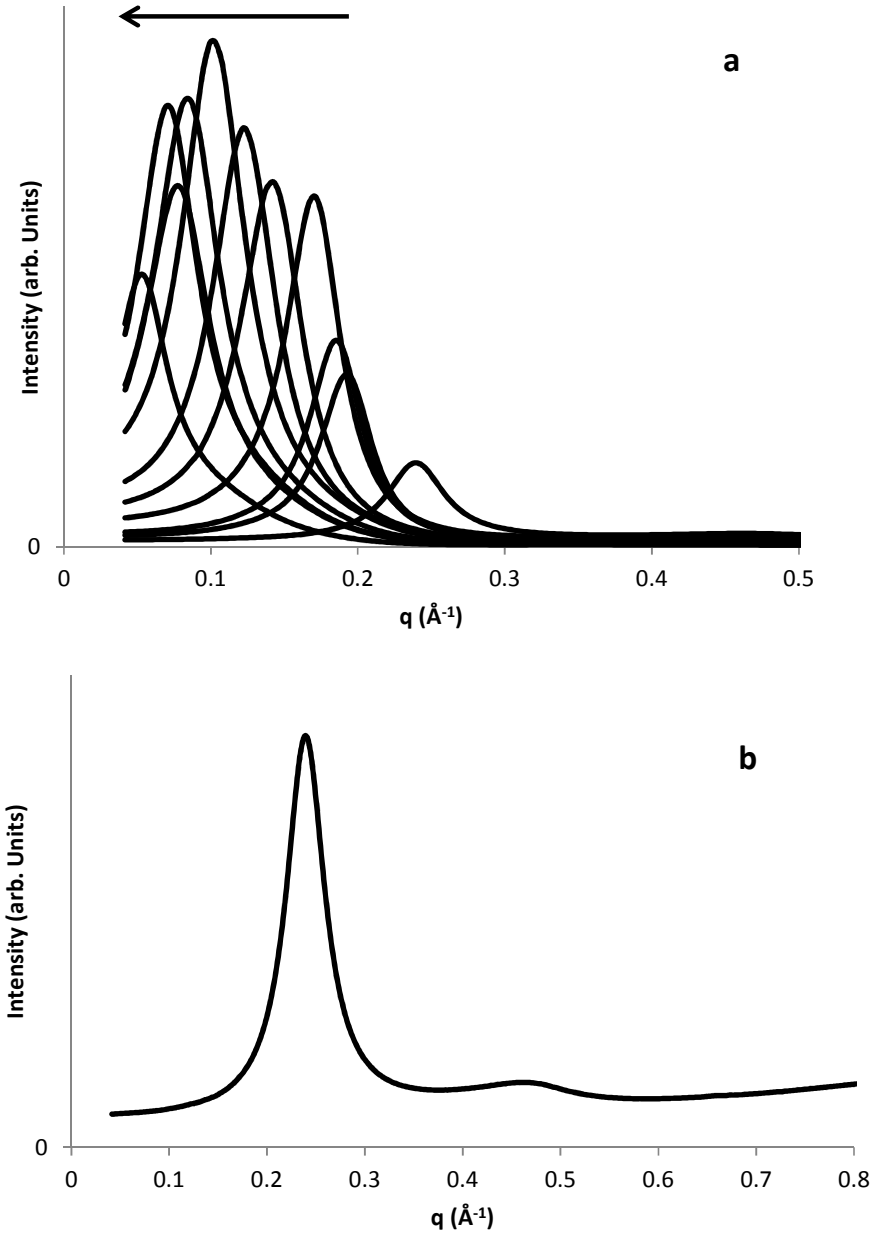

Figure 3. a) Stacked SAXS patterns for MImOF-water solutions with arrow indicating direction of increasing water content, with water contents of 10, 20, 25, 30, 40, 50, 60, 70, 75, 80 or 90 wt%. b) 90 wt% MImOF and 10 wt% water.

Tertiary MImOF-water-phytantriol systems

The SAXS/WAXS patterns and textures from CPOM were used to identify the lyotropic liquid crystal phases present for phytantriol in the neat MImOF and MImOF-water solutions over the temperature

range from 25-70 °C. The phase diagrams for phytantriol in neat MImOF and MImOF with 10, 25, 50 and 75 wt% water are shown in Figure 4. The corresponding SAXS/WAXS patterns at 25 °C are provided in the supplementary material Figure S1.

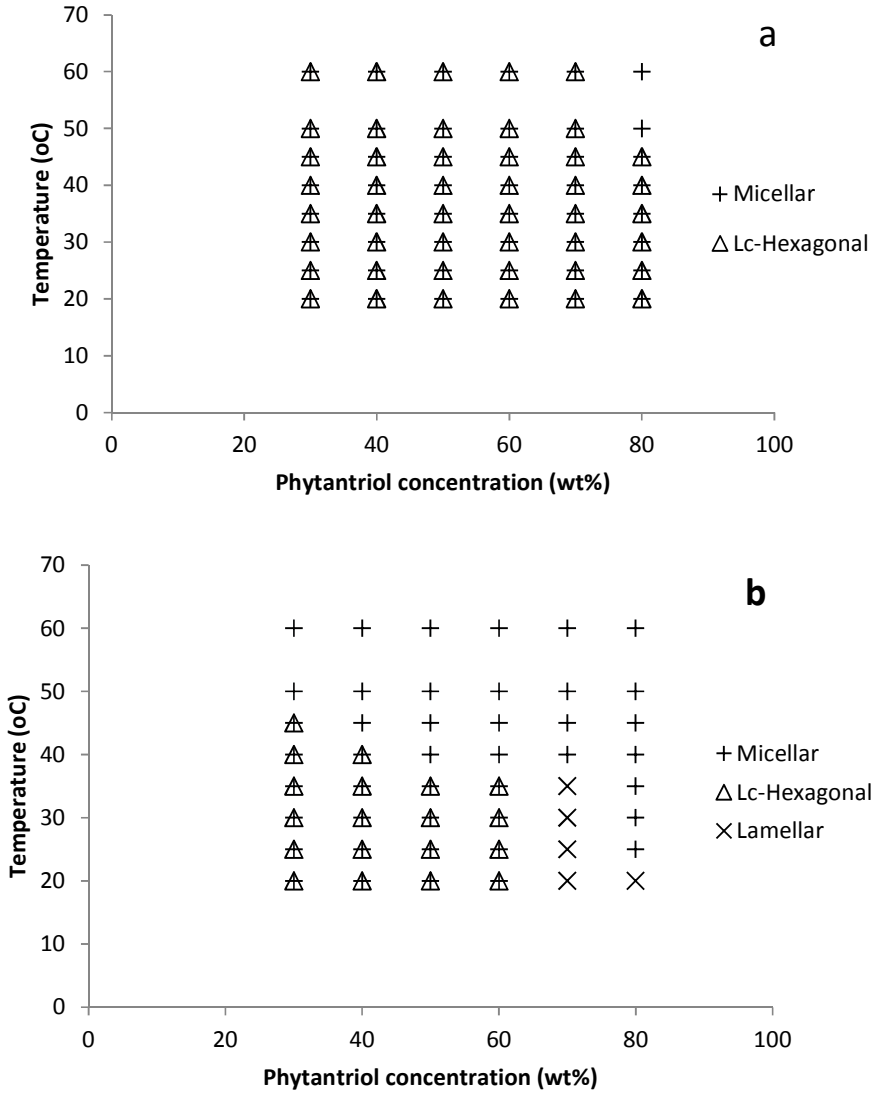

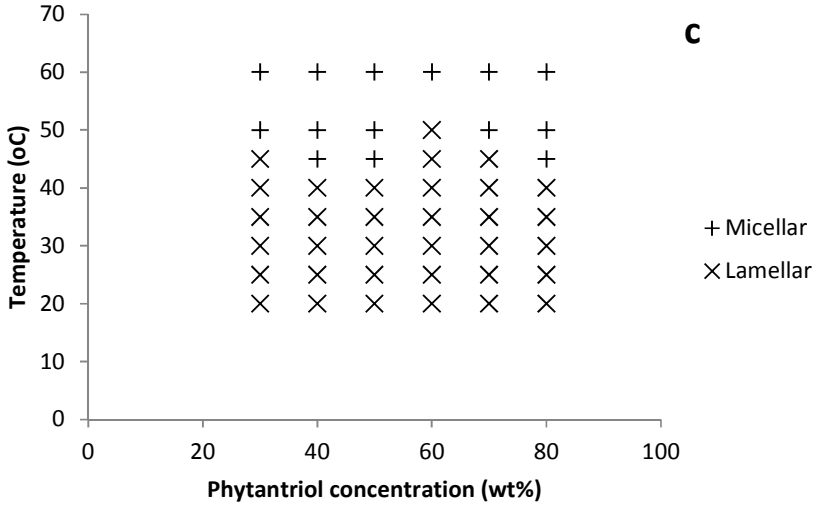

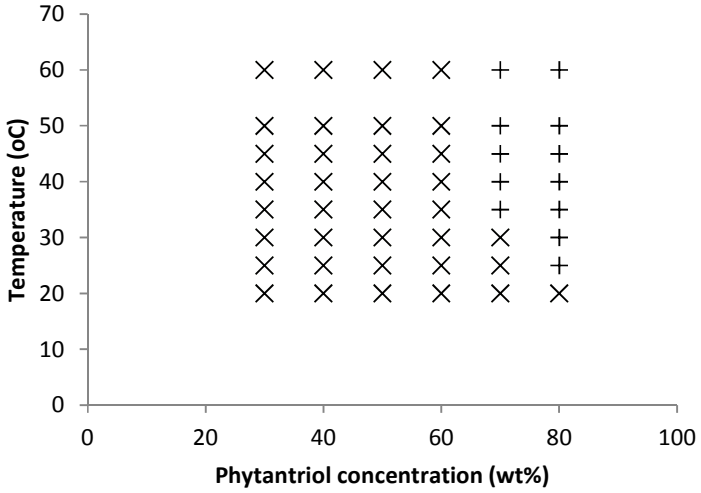

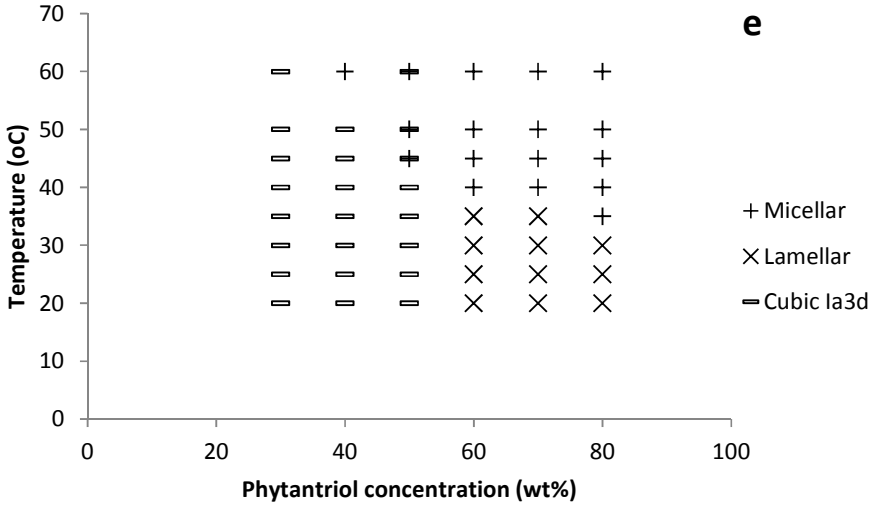

Figure 4. Phase diagrams phytantriol in a) MImOF (no water), b) MImOF90wt%-water10wt%, c) MImOF75wt%-water25wt%, d) MImOF50wt%-water50wt% and e) MImOF25wt%-water75wt%. Lc- denotes a crystalline phase.

The crystalline phase denoted Lc-hexagonal was present in neat MImOF and MImOF with 10 wt% water. This phase was attributed to that of the neat MImOF. The d-spacing had negligible change with increasing phytantriol or temperature and all values were between 20.7 and 20.9 Å. For the non-crystalline samples there were no apparent peaks from the solvents in the SAXS patterns.

The classification of samples as lamellar or micellar was determined based on the SAXS/WAXS patterns in addition to CPOM[1]. The SAXS patterns for 40 wt% phytantriol in MImOF75wt%-water25wt% are shown in Figure 5 for the transition from lamellar to micellar with increasing temperature. The broad peaks were assigned as micellar since their shape was indicative of a fluid micellar phase, and their q position and shape in the scattering pattern, and location in the phase diagram were consistent with those assigned as micellar in Barauskas et al. for the closely related phytantriol-water system.[1] The corresponding lamellar texture for the same sample under cross polarised optical microscopy (CPOM) is shown in Figure 6 at 30 ^{o}C. The micellar phase present at higher temperatures is isotropic under CPOM.

It is evident from Figure 5 that there is a slight shift of the lamellar peak to higher q values with increasing temperature, until it melts completely by 45 ^{o}C. This shift corresponds to a decrease in the lattice d-spacing, as shown in Figure 7. This was consistent for all the samples studied. Similarly, there was a decrease in the d-spacing with increasing phytantriol concentration, which indicates that increasing the solvent proportion causes a swelling of the lamellar phase.

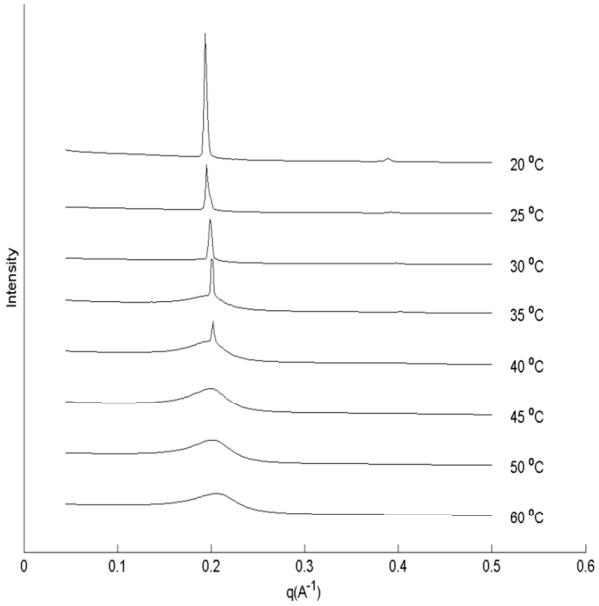

Figure 5. Combined SAXS/WAXS diffractograms highlighting the lamellar to micellar transition for a formulation of 40 wt% phytantriol in a solution of MImOF75wt%-water25wt% .

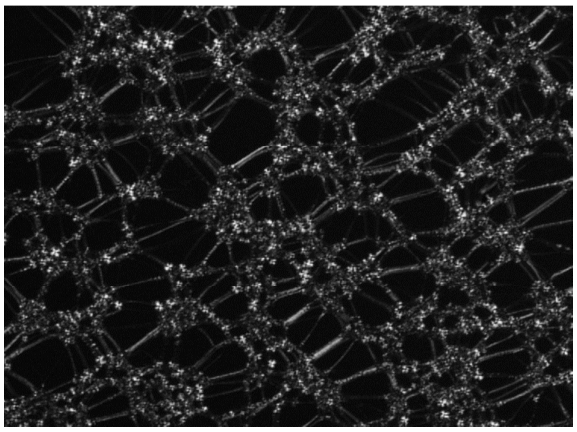

Figure 6. Representative CPOM image of for 40wt% phytantriol in MImOF75wt%-water25wt% at 30 ^{o}C, which exhibits features characteristic for a lamellar phase.

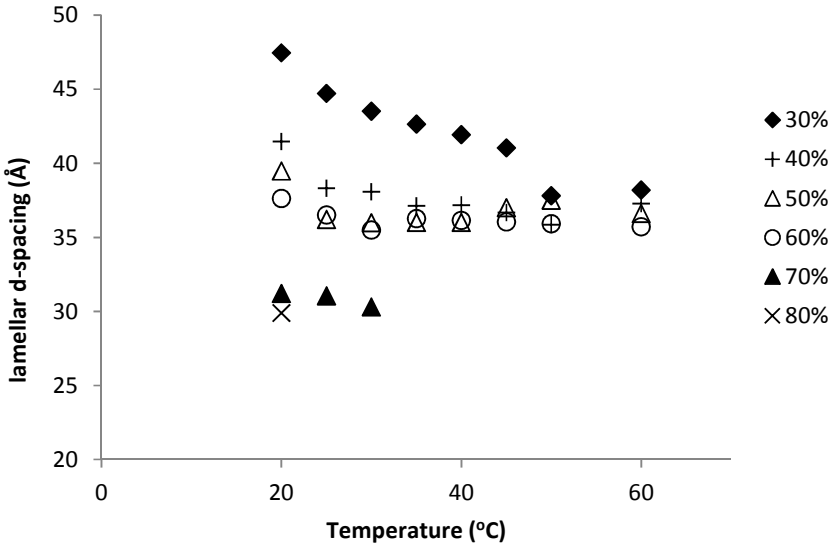

Figure 7. Changes in d-spacing of the lamellar phase of a formulation of phytantriol in a solution of MImOF50wt%-water50wt%. The concentrations refer to the total phytantriol wt% in the tertiary system.

Phytantriol was only observed to form a cubic phase in the solvent system with the least concentration of MImOF in the study, MImOF 25 wt%-water 75 wt%, and only for 30, 40 and 50 wt% of phytantriol, as shown in Figure 4e. A representative SAXS pattern of this cubic phase is provided in Figure 8 and it indexed well as an Ia$\bar{3}$d phase. It has been categorised as an inverse phase based on its

position in the lyotropic liquid crystal phase sequence, and the phytantriol-water phase diagram previously reported.[1] The lattice spacing varied between 100 and 140 Å, decreasing with increasing temperature, and decreasing with increasing phytantriol concentration. In comparison, Barauskas et al. reported that the Ia$\bar{3}$d cubic phase in phytantriol-water had a lattice parameter between 86-100 Å.[1] The significantly larger lattice spacing with the addition of MImOF has been attributed to greater swelling of the cubic phase, and has previously been observed for phytantriol-water with the addition of distearoylphosphatidylglycerol (DSPG)[18].

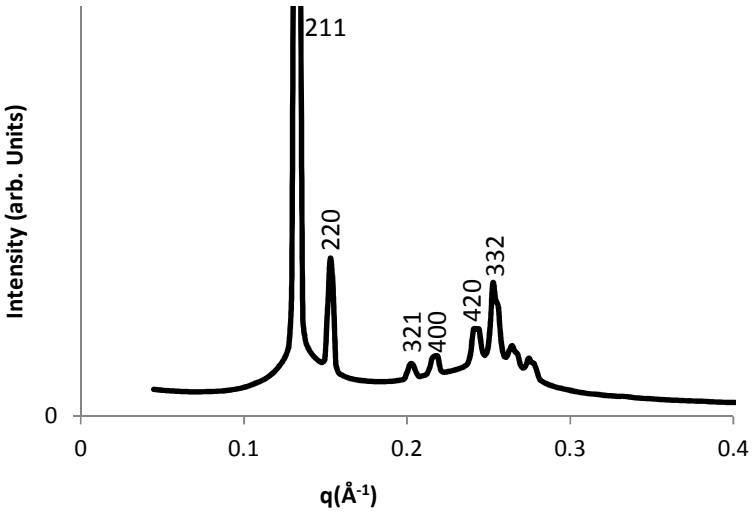

Figure 8. SAXS patterns for cubic Ia$\bar{3}$d for the formulation 40 wt% phytantriol in MImOF25wt%-water75wt% solution equilibrated at 20 ^{o}C. The first peak has been truncated to aid in the viewing of the less intense peaks.

Infrared Spectroscopy

The IR spectra were recorded for all the samples at room temperature, and these have been provided in the supporting material Figure S2. Characteristic bands in the IR have been selected which provide information about the bonding predominantly associated with the phytantriol, FPIL cation or anion. Previously the interaction of water at low concentrations in aprotic ILs containing imidazolium cations with a variety of anions have been reported[24], and more recently for higher water concentrations [25,26]. The water in conventional PILs analogous to ethylammonium nitrate have previously been reported to form pools of bulk-like water.[6] We are not aware of IR previously being reported for ILs containing the OF anion, but it has been reported for perfluoroocatanoic acid.[29] Detailed IR and Raman information for phytantriol has also been previously reported.[23]

Table 1. Infrared spectroscopy band assignment.

Band (cm^{-1})	**Assignment**

2850-2950	C-H stretching mode (phytantriol)
3061	C2-H stretch (MIm^+)
3115	C4-H stretch (MIm^+)
3149	C5-H stretch (MIm^+)
~ 2947, 2963	$N\text{-}CH_3$ symm and asymm stretch (MIm^+)
1555	C=N stretch for C and N in the imidazolium ring, $N\text{-}CH_3$ (MIm^+)
1587	C=N stretch for C and N in the imidazolium ring, N-H (MIm^+)
1662	C=C stretch within imidazolium ring (MIm^+)
1680	C=O vibration (OF^-)
1125-1237	C-F stretches (OF^-)

Phytantriol bands

The C-H stretching modes for the phytantriol were present between 2850 and 2950 cm^{-1}. There was negligible peak position change with changing MImOF or water concentration, and the representative series of phytantriol in 75 wt% MImOF-25 wt% water has been provided in Figure S3 of the supporting material. This may indicate that the alkyl component of the phytantriol is segregating to form the lyotropic liquid crystal phases, and not interacting with the MImOF ions. Above 3000 cm^{-1} the predominant contributions are from water and the OH on phytantriol. These peaks are broad and highly overlapping, and it was not possible to deconvolute them.

MIm cation

The MIm^+ cation had distinguishable bands in the IR which provided information about the key components of the cation, as shown in Table 1. The following discussion uses the numbering of the carbon and nitrogen atoms in the imidazolium ring as shown in Figure 1.

The C-H stretching vibrations were difficult to distinguish for some of the samples due to its colocation with the broad OH peaks from water and phytantriol. However, for many samples the C-H stretching vibrations could be clearly distinguished. The IR spectra for MImOF-water without phytantriol are shown in Figure 9 between 3000 to 3250 cm^{-1}. It is evident that the three MIm^+ peaks rapidly reduce in intensity with increasing water content, and that all three undergo a blue shift, though this was very small for C4-H. The C2-H and C5-H stretches shifted by 21 and 10 cm^{-1} respectively with addition of 30 wt% water. This is consistent with what has previously been reported for EMIm ethylsulfate with water [26]. These blue shifts are arising due to a weakening of the hydrogen bond from the C-H, and hence indicates the C-H...anion bond is weakening.

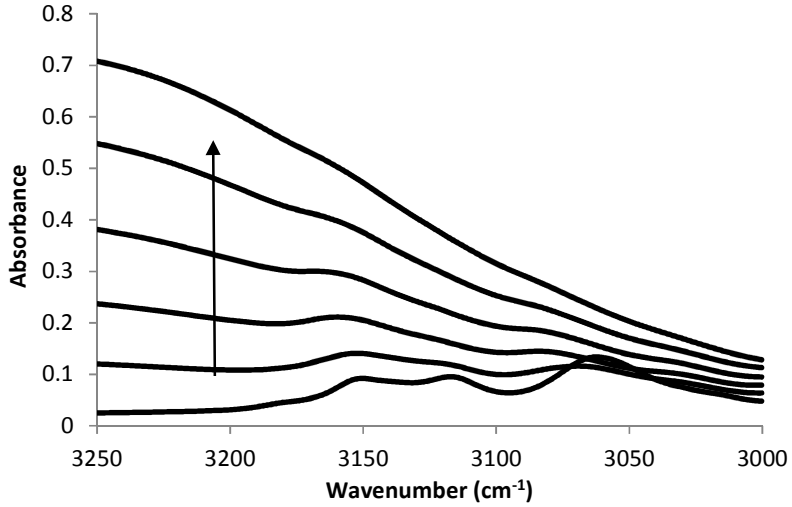

Figure 9. Stacked IR spectra showing the C-H bands between 3000 and 3200 cm^{-1} for neat MImOF, bottom, and increasing water in the direction of the arrow for formulations with10, 20, 30, 50 and 75 wt% water.

Another region of the IR spectra which was utilised to investigate the interaction of the components in the ternary mixtures were the C=N and N-H stretching frequencies of the imidazolium ring located in the cation of FPIL. The two nitrogen atoms in the imidazolium ring behaved very differently due to their different substitution with either a methyl or hydrogen substituent. N1-H, stretching frequency with the hydrogen substituent, underwent significant change with addition of water, with the C=N stretch shifting from 1587 cm^{-1} for MImOF to higher wavenumbers by ~4 cm^{-1} on addition of 10 wt%, and then little further change with greater proportions of water, shown in Figure 10. It is proposed that the water is strongly interacting though hydrogen bonds with the available hydrogen, and forming a stronger interaction than is present between the cation and anion. Above 10 wt% it is envisaged that the N-H sites would all be interacting with water, hence further addition of water have little effect. In contrast, the C=N for N2 with a methyl substituent at 1555 cm^{-1} had negligible change in peak position with addition of water or phytantriol, shown in Figure 10. Though it should be noted that the symmetric and asymmetric stretch of the N-CH_3 at around 2947 and 2963 respectively were weak in intensity, and no conclusions could be drawn due to the inability t to distinguish them from the broad OH contribution for formulations with water content greater than 40 wt%. Both the C=N bands had negligible shifts with addition of phytantriol.

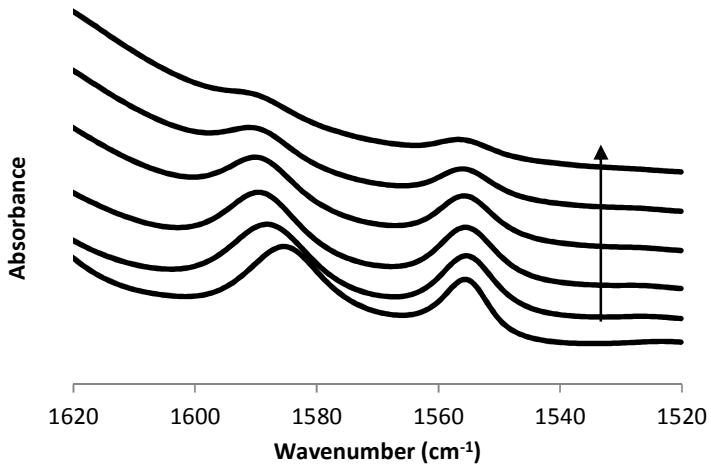

Figure 10. Stacked IR spectra showing the C=N bands of the imidazolium cation between 1520 and 1620 cm^{-1}. Neat MImOF, bottom, and increasing water in the direction of the arrow for formulations with10, 20, 30, 50 and 75 wt% water. C=N1 is present at ~1587 cm^{-1} and C=N2 at ~1555 cm^{-1}. The spectra have been offset to aid in viewing.

OF anion

The most informative IR band associated with the OF anion is the C=O vibration at approximately 1680 cm^{-1}. In the neat IL the C=O is significantly hydrogen bonded to the cation. However, on addition of water or phytantriol this hydrogen bond between the cation and the anion is weakened, which is shown in Figure 11. There is a significant increase in the wavenumber on addition of 10 wt% water, which we suggest is due to the C=O contributing a second peak at ~1640 cm^{-1} in conjunction with the shifting of the original peak at around 1680 cm^{-1}. This blueshift of the C=O band corresponds to strengthening the C=O bond, and hence a weakening of the hydrogen bond to the cation.

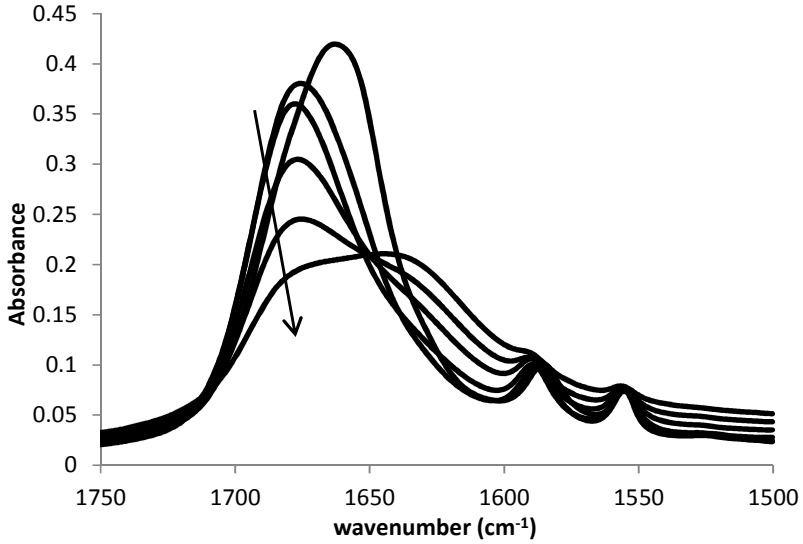

Figure 11. Stacked IR spectra showing the C=O band at approximately 1680 cm^{-1}, with neat MImOF, top, and increasing formulations with increasing water content in the direction of the arrow for 10, 20, 30, 50 and 75 wt% water.

When the phytantriol is added to neat MImOF then there is a similar change in the C=O vibration, with an increase in the wavenumber with increasing phytantriol concentration. However, this increase is less pronounced than is seen with water. We suggest that this different rate is due to the larger phytantriol being less able to interact with the C=O bond due to steric factors compared to water,and that a 10 wt% increase for water has a far greater number of molecular species than a 10 wt% increase for phytantriol. No effect is observed on adding phytantriol to MImOF with 10 wt% water or more present. It appears that the phytantriol will form hydrogen bonds with MIm^{+}, though when water is present the water interaction will dominate the hydrogen bonding with the cation and phytantriol prefers self segregation.

The C-F stretches contribute several bands to the IR spectra between 1125-1237 cm^{-1}. On addition of water the intensity of all these bands decreased as expected due to dilution, and the IR spectra for MImOF and water are shown in Figure 12a. The bands at 1125 and 1138 cm^{-1} decreased in intensity more significantly compared to the other bands. The band at 1191 cm^{-1} either shifts to higher wavenumber with increasing water, with an increase in 10 cm^{-1} by 75 wt% added water, or decreases in intensity with the peak at 1200 cm^{-1} becoming more prominent. Overall, this shows that the OF groups are influenced to some extent by the addition of water. There may be some carboxyl groups of OF anions which were hydrogen bonded to other OF anions which are being replaced by water. The IR spectra suggest that there are some fluorine sites more accessible to the water, due to certain IR bands in this region being affected more than others.

The C-F stretches for 30 wt% phytantriol in the different MImOF-water compositions are shown in Figure 12b. Addition of phytantriol to MImOF, or MImOF-water led to a decrease in intensity which was consistent across all the bands, and suggests that there may be little bonding/interaction between the fluorine in the OF and the phytantriol. The top two traces correspond to the MImOF being in a crystalline state, and it appears that in the non-crystalline state the peak at 1191 cm^{-1} has a significant reduction in intensity. All the phytantriol-MImOF-water compositions where the samples were non-crystalline showed very little difference in the peak positions, though did have some changes in the intensities due to dilution effects. A representative plot for phytantriol in 50 wt% MImOF – 50 wt% water is provided in Figure S4 of the supporting material. This suggests that there may be little bonding/interaction between the fluorine in the OF and the phytantriol. However, it is possible that there is mixing of the fluorocarbon and phytantriol chains.

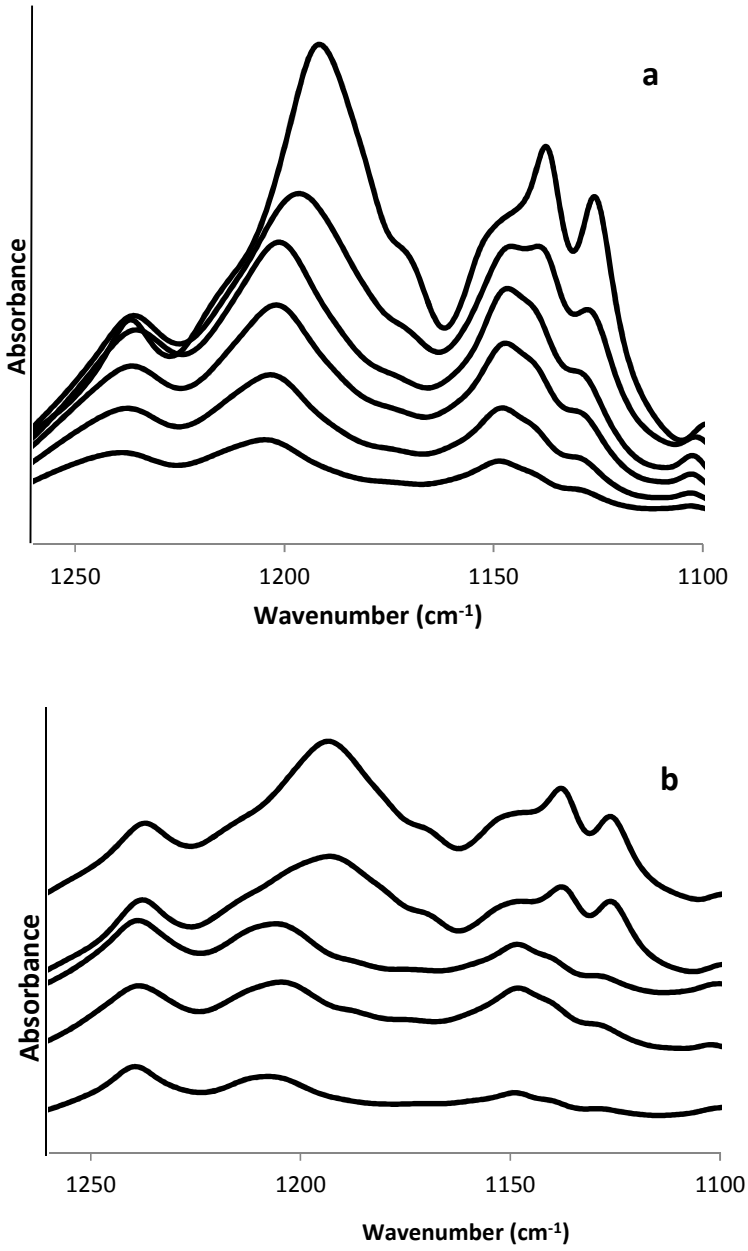

Figure 12. IR plot showing the changes in the C-F bands for samples containing a) MImOF and water, where the top trace corresponds to neat MImOF, and in decreasing intensity there is 10, 20, 30, 50 and 75 wt% water present. b) stacked plot of 30 wt% phytantriol on changing the MImOF and water proportions. The top trace corresponds to 30 wt% phytantriol in the solvent of neat MImOF, subsequent ones have solvent mixtures of MImOF-water with 10, 25, 50 and 75 wt% water respectively. Note that in (a) the changes in intensity are due to dilution effects, whereas in (b) the traces have been offset to aid in viewing.

Discussion

It is evident from the IR spectroscopy that the water is preferentially forming hydrogen bonds with the MIm cation, predominately at the N-H site. This leads to a decrease in the hydrogen bonding between the MImOF cation and anion, with a significant impact on the long range order and structure of the sample, which can be observed from the SAXS/WAXS patterns shown in Figure 2. More detailed investigations into the role of water on the FPILs will be reported in the future.

Increasing the proportion of MImOF in the phytantriol-water-MImOF tertiary system decreased the liquid crystal phase diversity. The phase diagram for phytantriol-(MImOF 25 wt%-water 75 wt%), shown in Figure 3e, is the one most similar to the phytantriol-water phase diagram reported by Barauskas et al.[1], although with less phase diversity. Unlike for the binary phytantriol-water system, there is no $Pn\bar{3}m$ cubic phase, and no evidence of an inverse hexagonal lyotropic liquid crystal phase in the concentration or temperature ranges investigated. CPOM investigations to higher temperatures (110 ^{o}C) did not show any evidence of a hexagonal phase. It is possible that decreasing the phytantriol concentration may lead to the formation of the $Pn\bar{3}m$ phase. The $Ia\bar{3}d$ cubic phase which was present was stable to a higher temperature than in neat water, while the lamellar phase was similar in its thermal stability range.

Increasing the MImOF concentration relative to water to between 50 and 90 wt% led to only the lamellar phase being supported, and the concentration and thermal stability range of the lamellar phase decreased with increasing MImOF. This indicates that the presence of the MImOF is increasing the effective head group area of the phytantriol through the presence of the bulkier ions of MImOF, which will lead to the lower curvature phases, and is consistent with the preference of the water to hydrogen bond with the MIm cation compared to the phytantriol head groups. Similar behaviour has previously been observed for tertiary systems of phytantriol-water with added glycerol[30] or propylene glycol[18]. The addition of glycerol caused hexosomes of phytantriol in water to go from an inverse hexagonal to water-in-oil microemulsion.[30] This indicates that some of the glycerol is penetrating into the hexosomes, and that the head group hydration of the phytantriol is decreasing due to the water hydrating the glycerol in addition to the phytantriol headgroups. Therefore the effective headgroup area is decreasing, and the curvature is more negative, similar to raising the temperature.[30] There was a lamellar phase present at room temperature for additions of propylene glycol less than 30 wt% (and approximately 60-94wt% phytantriol and 7-20wt% water). The cubic phases of $Pn\bar{3}m$ and $Ia\bar{3}d$ were retained for only up to 10 wt% propylene glycol.[18]

Conclusion

The tertiary phase system of MImOF, water and phytantriol was investigated. It was observed that increasing the proportion of MImOF led to less lyotropic liquid crystal phase diversity, lower curvature phases, and smaller thermal and concentration stability regions for the phases. Phytantriol was able to form lyotropic liquid crystal phases in the solvent system of water with at least 75 wt% MImOF. Lamellar phases were present for MImOF concentrations between 25 and 90 wt% relative to water. The inverse hexagonal and $Pn\bar{3}m$ cubic phases which are present in phytantriol-water were not observed for the concentrations of MImOF used. A cubic $Ia\bar{3}d$ phase was only observed when the MImOF concentration was 25 wt% relative to water. This cubic phase had a significantly larger lattice spacing when MImOF was present, indicating the MImOF is swelling the cubic phase.

FT-IR spectra of the MImOF-water and phytantriol-MImOF-water systems were characterised, and infrared marker bands for intermolecular interactions were specified. It was evident that the water is forming hydrogen bonds with the MIm cation, particularly at the N-H site, and that this is weakening the hydrogen bond between the cation and the anion of MImOF.

The nanostructure of the neat MImOF is complex, containing hydrocarbon, fluorocarbon and polar domains which are forming through segregation of the alkyl and fluorocarbon chains into separate domains. The development of ILs for niche applications will be aided by understanding how they interact with solutes. In this investigation we have shown that the addition of water to the MImOF has a pronounced effect on the liquid structure present. The complex system of the phytantriol-MImOF-water has multiple hydrogen bonds and other interactions which are present. The use of IR spectroscopy highlighted the way that these are modified for different phytantriol, water and MImOF proportions.

References

(1) Barauskas, J.; Landh, T. *Langmuir* **2003**, *19*, 9562.

(2) Greaves, T. L.; Drummond, C. J. *Chemical Reviews* **2008**, *108*, 206.

(3) Canongia Lopes, J. N.; Padua, A. A. H. *Journal of Physical Chemistry B* **2006**, *110*, 3330.

(4) Atkin, R.; Warr, G. G. *Journal of Physical Chemistry B* **2008**, *112*, 4164.

(5) Greaves, T. L.; Kennedy, D. F.; Mudie, S. T.; Drummond, C. J. *Journal of Physical Chemistry B* **2010**, *114*, 10022.

(6) Greaves, T. L.; Kennedy, D. F.; Weerawardena, A.; Tse, N. M. K.; Kirby, N.; Drummond, C. J. *J. Phys. Chem. B* **2011**, *115*, 2055.

(7) Hayes, R.; Imberti, S.; Warr, G. G.; Atkin, R. *Angewandte Chemie (International ed. in English)* **2012**, *51*, 7468.

(8) Greaves, T. L.; Kennedy, D. F.; Kirby, N.; Drummond, C. J. *Phys. Chem. Chem. Phys.* **2011**, *13*, 13501.

(9) Greaves, T. L.; Drummond, C. J. *Chem. Soc. Rev.* **2013**, *42*, 1096.

(10) Chen, Z.; Greaves, T. L.; Caruso, R. A.; Drummond, C. J. *J. Mater. Chem.* **2012**, *22*, 10069.

(11) Shen, Y.; Kennedy, D. F.; Greaves, T. L.; Weerawardena, A.; Mulder, R. J.; Kirby, N.; Song, G.; Drummond, C. J. *Phys. Chem. Chem. Phys.* **2012**, *14*, 7981.

(12) Russina, O.; Lo Celso; Di Michiel, M.; Passerini, S.; Appetecchi, G. B.; Castiglione, F.; Mele, A.; Caminiti, R.; Triolo, A. *Faraday Discussions* **2013**, *DOI: 10.1039/c3fd00056g*.

(13) Greaves, T. L.; Kennedy, D. F.; Shen, Y.; Hawley, A.; Song, G.; Drummond, C. J. *Phys. Chem. Chem. Phys.* **2013**, *15*, 7592.

(14) de Campo, L.; Varslot, T.; Moghaddam, M. J.; Kirkensgaard, J. J. K.; Mortensen, K.; Hyde, S. T. *Phys. Chem. Chem. Phys.* **2011**, *13*, 3139.

(15) Evans, D. F.; Yamauchi, A.; Roman, R.; Casassa, E. Z. *Journal of Colloid and Interface Science* **1982**, *88*, 89.

(16) Greaves, T. L.; Weerawardena, A.; Fong, C.; Drummond, C. J. *Langmuir* **2007**, *23*, 402.

(17) Wijaya, E. C.; Greaves, T. L.; Drummond, C. J. *Faraday Discussions* **2013**, *DOI: 10.1039/c3fd00077j*.

(18) Wadsten-Hindrichsen, P.; Bender, J.; Unga, J.; Engstrom, S. *Journal of Colloid and Interface Science* **2007**, *315*, 701.

(19) Dong, Y. D.; Dong, A. W.; Larson, I.; Rappolt, M.; Amenitsch, H.; Hanley, T.; Boyd, B. J. *Langmuir* **2008**, *24*, 6998.

(20) Greaves, T. L.; Weerawardena, A.; Fong, C.; Drummond, C. J. *Journal of Physical Chemistry B* **2007**, *111*, 4082.

(21) Greaves, T. L.; Weerawardena, A.; Krodkiewska, I.; Drummond, C. J. *Journal of Physical Chemistry B* **2008**, *112*, 896.

(22) Mulet, X.; Kennedy, D. F.; Greaves, T. L.; Waddington, L. J.; Hawley, A.; Kirby, N.; Drummond, C. J. *Journal of Physical Chemistry Letters* **2010**, *1*, 2651.

(23) Misiunas, A.; Niaura, G.; Talaikyte, Z.; Eicher-Lorka, O.; Razumas, V. *Spectrochimica Acta Part a-Molecular and Biomolecular Spectroscopy* **2005**, *62*, 945.

(24) Cammarata, L.; Kazarian, S. G.; Salter, P. A.; Welton, T. *Phys. Chem. Chem. Phys.* **2001**, *3*, 5192.

(25) Zhang, Q. G.; Wang, N. N.; Wang, S. L.; Yu, Z. W. *Journal of Physical Chemistry B* **2011**, *115*, 11127.

(26) Zhang, Q. G.; Wang, N. N.; Yu, Z. W. *Journal of Physical Chemistry B* **2010**, *114*, 4747.

(27) Kirby, N.; Boldeman, J. W.; Gentle, I.; Cookson, D. In *Synchrotron Radiation Instrumentation, Pts 1 and 2*; Choi, J. Y., Rah, S., Ed.; Amer. Inst. Physics: Melville, 2007; Vol. 879, p 887.

(28) Kirby, N.; Mudie, S. T.; Hawley, A.; Cookson, D. J.; Mertens, H. D. T.; Cowieson, N.; Samardzic-Boban, V. *J. Appl. Cryst.* **2013**, *46*, 1670.

(29) Li, X.; Zhang, P.; Jin, L.; Shao, T.; Li, Z.; Cao, J. *Environ. Sci. Technol.* **2012**, *46*, 5528.

(30) Engelskirchen, S.; Maurer, R.; Glatter, O. *Colloids and Surfaces a-Physicochemical and Engineering Aspects* **2011**, *391*, 95.

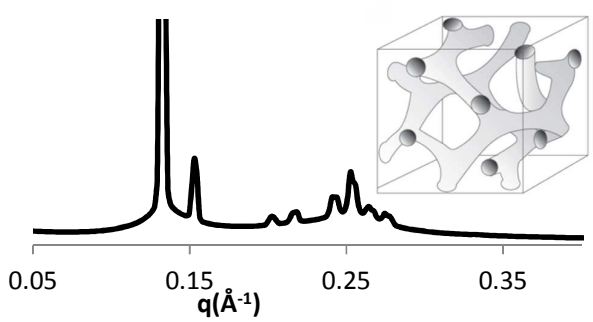

Liquid crystal phases of phytantriol supported in solvent mixtures of a fluorinated protic ionic liquid and water